# Experimental Study and wake Characteristics Comparison of a Car Model in Steady and Unsteady Flow

**V. Barzanooni**
Department of Mechanical Engineering,
Hakim Sabzevari University
E-mail: v.barzanooni@gmail.com

**A. B. Khoshnevis**\*
Department of Mechanical Engineering,
Hakim Sabzevari University
E-mail: Khosh1966@yahoo.com
\*Corresponding author

**Abstract:** In this study, changes in velocity, turbulence intensity and drag coefficient in the wake of a notch-back car modelling steady and unsteady flow is measured and evaluated. The blow open circuit wind tunnel is used to simulate fluid flow. Turbulence intensity and nominal maximum speed of the device is measured to be 0.01% and 30m/s, respectively. The speed has been continuously increased by an inverter causing changes in rotational speed of the electromotor. In the near location to the model, the results showed three different regimes in the velocity profile of the model's wake. With increasing distance from the model and with increasing the speed, three regimes in the wake are close to each other. Drag coefficient for several velocities is measured, where the result shows that decreasing in drag coefficient is proportional with increasing velocity. In addition, the changing trends of higher order velocity of parameters like flatness and skewedness are depicted.

**Biographical notes: V. Barzanooni** is a PhD student at Faculty of Engineering of Hakim Sabzevari University, Sabzevar, Iran. **A. B. Khoshnevis** is an Associate Professor of Mechanical Engineering at Hakim Sabzevari University, Sabzevar, Iran. He received his PhD from Indian Institute of Technology of Madras Chennai (2000), India, MSc from Indian Institute of Technology of Madras Chennai (1995), and BSc from Ferdowsi University of Mashad, Iran (1990), all in mechanical engineering. His scientific interest includes experimental aerodynamics.

## 1   INTRODUCTION

Due to the fact that theoretical methods and calculations may be somewhat different from empirical engineering design, experimental methods using wind tunnel are often a useful technique to determine flow parameters such as models fluctuation. For this purpose, the present investigation deals with experimental study of the characteristics of the wake and drag coefficient changes of a car model in unsteady flow. In experimental methods using wind tunnel, a model, experiment facilities and measurement device are needed; hence such methods are usually more expensive than theoretical and numerical methods.

In numerical methods, governing equations on fluid flow are solved by several techniques. In these techniques, because of simplifications, occurrence of error in results due to turbulence modelling or boundary conditions is often possible. Therefore results of numerical methods should be compared and approved by experimental results and then codes may be verified if needed [1]. Various numerical and experimental studies have been carried out on several model cars. Basic investigations published until now have been about basic car models, namely square back and fast back models. For example Ahmed et al., built a simple car model and measured its rear window orientation in several iterations [2].

Some researchers like Gilli and Chometon or Hanaoka and Kiyohira simulated the above mentioned model numerically [3], [4]. Since the results published by Ahmed are limited, comparable criterion for numerical results were limited to drag coefficient. Gillieron and Spohn and Lienhart and Stoocks simulated these models in detail and obtained experimental results including velocity vectors and Reynolds numbers by means of LDA (Laser Doppler Anemometer) [5], [6]. Khalighi et al., obtained velocity profiles and turbulent intensity profiles for a car model experimentally [7]. Javaresh kian et al., studied the influence of some parameters on the drag coefficient [8]. Shayesteh tried to study a car model numerically, where Javareshkian et al., studied the same car model experimentally and numerically [9], [10]. Likewise Watkins and Vino studied variation of drag and lift coefficients for Ahmed's models in tandem arrangement [11].

Because most studies have been performed in steady flows, hence in this research flow characteristics in the wake of a car model in an unsteady flow (vehicle with constant acceleration) are measured and investigated. Furthermore, drag coefficient changes in an unsteady flow are investigated for the first time. The wind tunnel implemented is manufactured by Fara-Sanjesh-Saba Company, which measures fluctuations up to 30 KHz and the accuracy of probe traverse is about 0.1mm.

## 2   EXPERIMENTAL SETUP AND MESAUREMENT TECHNIQUE

Present experiments were carried out in an open circuit low-speed wind tunnel to simulate uniform air flow. This wind tunnel has a settling chamber with 4 series of mesh screen ($1mm^2$) and one honey comb, to make the uniform airflow.
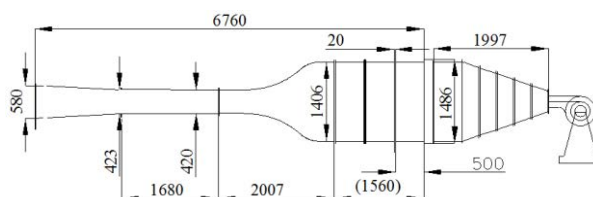


**Fig. 1**     Schematic view of the wind tunnel

The maximum wind tunnel speed is approximately 30 m/s, with 1800 mm length and $0.4{\times}0.4m^2$ test area cross-section. The free fluid turbulence intensity is less than 0.1%. The hotwire used in this study was CTA type, which was manufactured by Fara-Sanjesh-Saba Ltd. Schematic view of the wind tunnel is presented in Fig. 1.
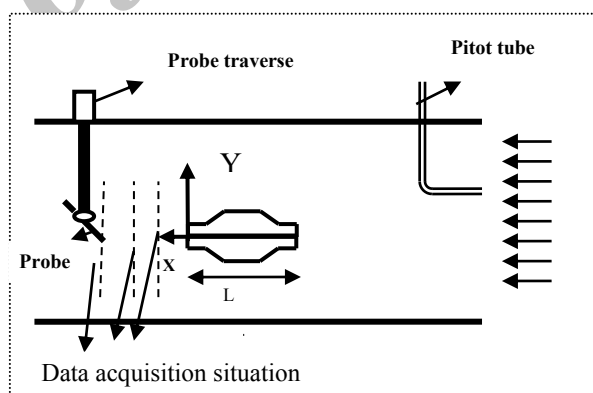


**Fig. 2**     Schematic view of the experimental apparatus

Input flow in these experiments first was increased from zero to 20 m/s in 20 seconds, and then experiments are performed in several steady velocities (5, 7.5, 10, 12.5, 15, 17.5, and 20 m/s). To increase the input flow velocity, an inverter is used. Inverter is a device that uniformly increases the fan speed of wind tunnel with respect to the set time, therefore increases the speed of the input flow. Experimental model was a simplification of Peugeot 405 without details such as mirrors, wheels, and antenna. It is important to consider the blockage ratio in construction of these models. Suggested ratio for this model is less than 0.1, if the flow influence near the test section walls and on the model surfaces is to be neglected [10], [11].

With respect to the present experimental conditions, for each  model, 0.042 ratio and for the two models a ratio of 0.084  is chosen in this research, where the scale factor of the model decided to be 1/75. Subsequently, the data acquisition took place at distances of X/L=0.01, 0.5, 1, and 2, behind the model at the heights of Y=-25, -20, -19, -18…0, 1, 2…20, and 25mm (Fig. 2).

## 3   VALIDATION

In order to ensure the correct operation of the wind tunnel, the validation test was performed. For this purpose, the free stream flow was measured and it was observed that the velocity profile is uniform as shown in Fig. 3.
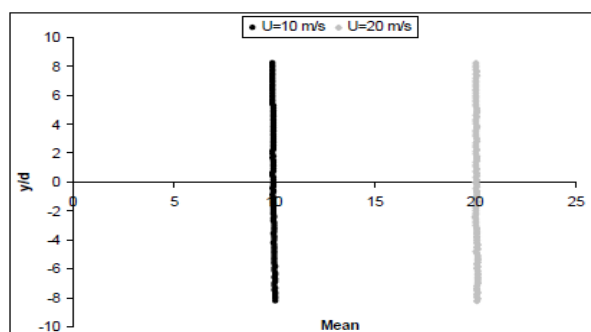


**Fig. 3**     Average speed fluctuation in the wind tunnel for speeds of 10 and 20 m/s
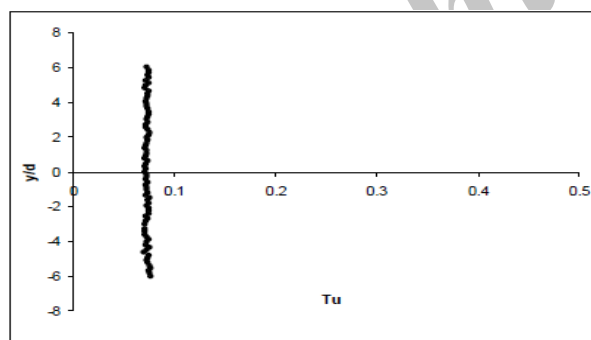


**Fig. 4**     Turbulence intensity variation in the wind tunnel at a speed of 10 m/s

Another experiment was conducted to measure the free stream turbulence intensity at different wind tunnel speeds (Fig. 4). According to the disturbance graphs of the wind tunnel test section, the turbulence intensity was investigated to be 0.08 %. Moreover, to survey the accuracy and performance of the wind tunnel and hot-wire anemometer, sample data was obtained and compared with the results claimed by other researchers.

However, due to the fact that there was no similar investigation in the literature on the chosen model, therefore a cubic cylinder model was used instead. Profile of the mean time of the longitudinal velocity component along the main stream ($\bar{U}$) for a sample cubic cylinder with aspect ratio of b/h=1 and Reynolds number of 8600, in two different sections is presented in Fig. 5. As it is observed in Fig. 5, a relatively good conformity exists between the present results and the results claimed by Saha et al., and also by Shadaram et al., where both have achieved the same Reynolds number [12], [13].
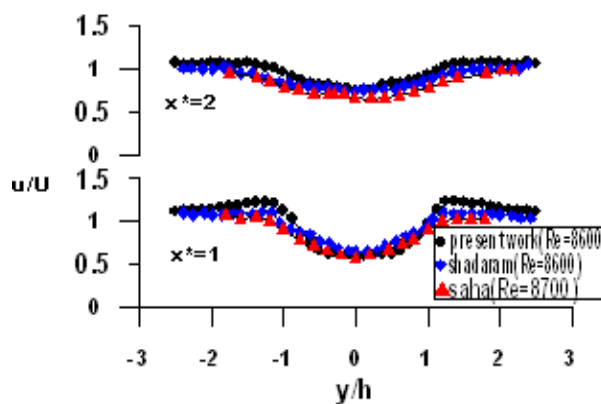


**Fig. 5**     Profile of mean velocity for a square cylinder in two different sections

## 4   WAKES-SURVEY EQUATIONS

The equations used to measure the drag force, can be simply derived from momentum and continuity equations. Chao, Antonia and Van Dam have conducted vast researches on the effect of turbulence intensity on drag coefficient measurement [14-16]. Van Dam obtained an equation to measure drag coefficient in which Reynolds tensions terms and flow intensity existed, but changes of flow density and viscous term were ignored [16]. The equation is:

$$C_d = \int \left( \frac{p_{s,a} - p_{s,w}}{q_\infty} \right) d\left( \frac{y}{l} \right) + 2\int \frac{\bar{u}}{U_\infty} \left( 1 - \frac{\bar{u}}{U_\infty} \right) d\left( \frac{y}{l} \right) - 2\int \frac{\overline{u'^2}}{U_\infty^2} d\left( \frac{y}{l} \right), \quad (1)$$

Including Pressure term:

$$\int \left( \frac{p_{s,a} - p_{s,w}}{q_\infty} \right) d\left( \frac{y}{l} \right),$$

Momentum term:

$$2\int \frac{\bar{u}}{U_\infty} \left( 1 - \frac{\bar{u}}{U_\infty} \right) d\left( \frac{y}{l} \right),$$

Reynolds tension:

$$2\int \frac{\overline{u'^2}}{U_\infty^2} d\left(\frac{y}{l}\right).$$

However, based on the analysis of Goldstein [17]:

$$p_{s,a} = p_{s,w} + \overline{q'}, \tag{2}$$

$$\overline{q'} = \frac{1}{2}\rho(\overline{u'^2} + \overline{v'^2} + \overline{w'^2}) \tag{3}$$

Substituting equation (3) into equation (1):

$$C_d = 2\int \sqrt{\frac{\overline{q}}{q_\infty}}\left(1 - \sqrt{\frac{\overline{q}}{q_\infty}}\right)d\left(\frac{y}{l}\right) + \frac{1}{3}\int \frac{(\overline{v'^2} + \overline{w'^2} + \overline{u'^2})}{U_\infty^2}d\left(\frac{y}{l}\right) \tag{4}$$

If: $u' = v' = w'$, then

$$C_d = 2\int \sqrt{\frac{\overline{q}}{q_\infty}}\left(1 - \sqrt{\frac{\overline{q}}{q_\infty}}\right)d\left(\frac{y}{l}\right) + \frac{1}{3}\int \frac{\overline{q'}}{q_\infty}d\left(\frac{y}{l}\right) \tag{5}$$

In which:

$$\overline{q'} = \frac{1}{2}\rho(\overline{u'^2} + \overline{v'^2} + \overline{w'^2}).$$

These equations may be used to determine drag coefficient in wind tunnel via Wake-Survey approach. Hence, Eq. (5) was used to measure drag coefficient in the present work.

## 5   RESULTS AND DISCUSSION

Figure 6 shows the free stream velocity at different time intervals 10 & 20 seconds that have been changed from 0m/s to 20m/s. In the first study, the velocity and turbulence intensity changes for different height and longitudinal positions, in the wake of model, with time and speed rise of the vehicle is referred, where the instantaneous velocity is shown in the twentieth second for three long positions in the wake. In the second phase of the study, the input flow rate of 20m/s was fixed High Order values of Velocity (skewness and kurtosis) and their maximum values in the wake were measured and evaluated.

Since, the frequency at the maximum amplitude is related to Von-Karman vortex frequency, hence its values for different longitudinal positions in the wake are shown. In addition, by displaying the mean velocity profiles for different inlet flow velocity drag coefficient, and how to change it at different speeds were investigated. Figures 8 to 10 show the velocity variations in the wake of model in the timeframe 0 to 20 seconds, and for wake different situations. Velocity in the wake, at y=3mm to y=9mm is very softly and its maximum for these positions is about 8m/s. In these positions a negligible deceleration in the interval 6 to 9 seconds can be seen. However, this deceleration is much more intuitive position, y=1mm and in the positions y= 13mm or more, this decrease is not observed, and the increasing speed process continues uniformly. At the position of x/L=0.01, following the fifth second, three different regimes can be distinctly observed.
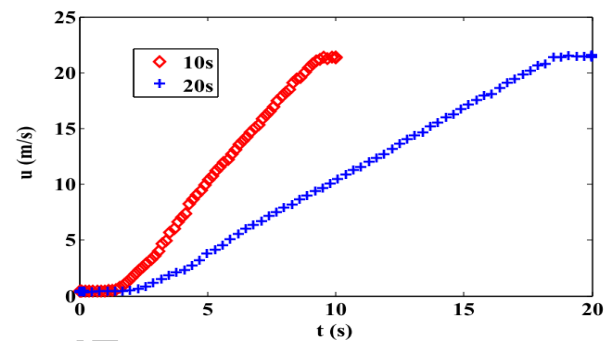


**Fig. 6**   Freestream unsteady velocity at different time

In the first regime, which corresponds to the measured position, y=3 mm and y=9mm, Gradient increase in speed with time is negligible. In the second regime, which corresponds to the positions y=1mm, and 11mm, the velocity increasing gradient is slightly increased. And ultimately speed at the end of time interval is nearly 15m/s. In the third regime, for positions: y=13, 15, 17, and 19mm, the gradient of velocity increasing is more, specifically for the positions y=17, and 19mm similar gradient of increasing of free flow velocity that is outside of the wake region model. With take distance from the model and in the position x/d=0.5, the three regimes are close to each other and gradient increase speed is increased at lower position.

**Table 1**   Magnitude of Velocity Fluctuation for steady and unsteady flow in different position at (19.9-20s)

| | $u'_{avg}(\frac{m}{s})$ | | | |
| --- | --- | --- | --- | --- |
| | Steady flow | | Unsteady flow | |
| | y=9mm | y=19mm | y=9mm | y=19mm |
| X/L = 0.01 | 0.01 | 0.015 | 5.25 | 12.65 |
| X/L = 0.5 | 0.01 | 0.124 | 9.84 | 11.2 |
| X/L = 1 | 0.03 | 0.041 | 10.0 | 10.05 |
| X/L = 2 | 0.17 | 0.144 | 9.94 | 9.52 |
| X/L = 4 | 0.03 | 0.194 | 10.1 | 10.82 |

Of course in the timeframe of less than 7 seconds, there is no difference in the velocity of the model wake. And with increasing time and free stream velocity, the velocity in the wake of model and in different height positions, increases with different gradients. It is necessary to explain that at X/L=0.5 positions, velocity increasing gradient is equal at different height positions. But at any moment, velocity at the higher position is different with other positions where this difference is due to the drop in velocity ranged from 7 to 10 seconds for the lower position. But in the location X/L=0.01, the velocity increasing gradient in various height positions is different.
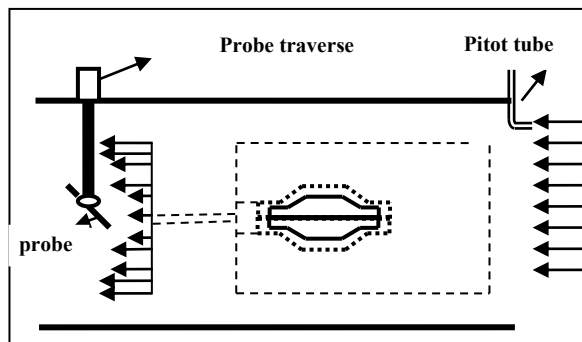


**Fig. 7**   Schematic view of the control volume
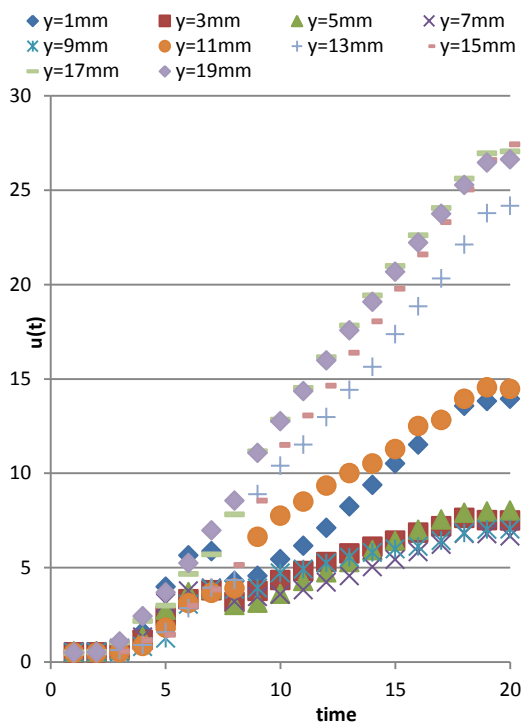


**Fig. 8**   Velocity change in the wake of model in the timeframe 0 to 20 seconds (X/L=0.01)
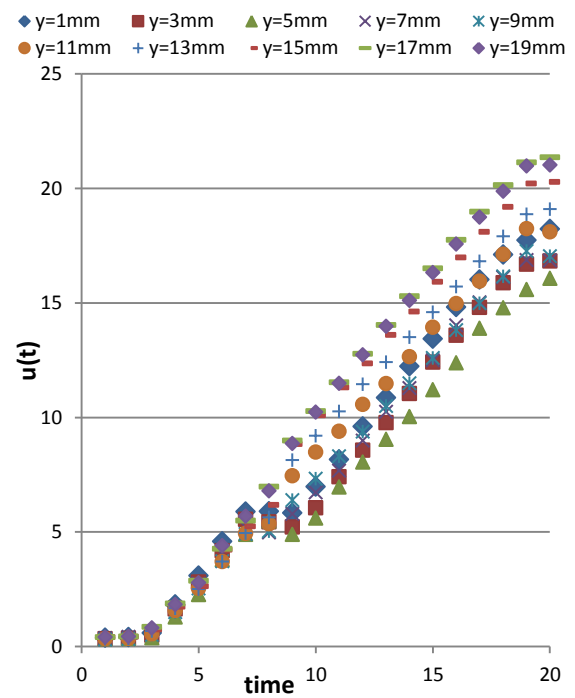


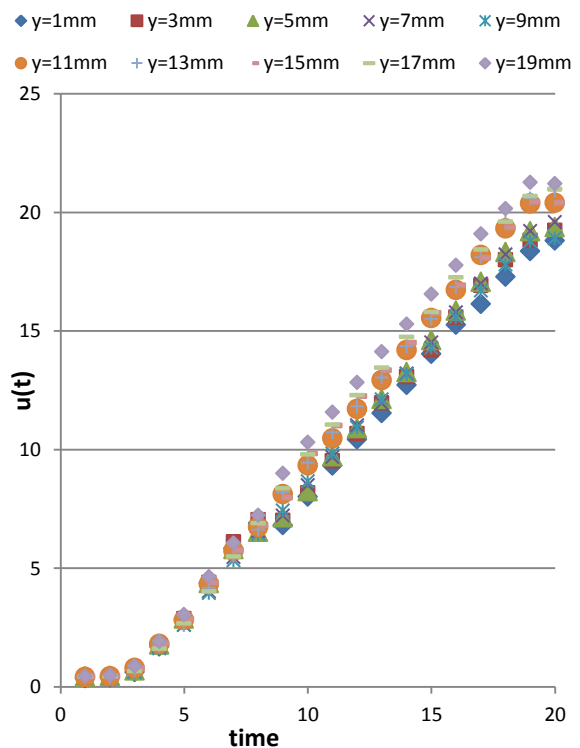**Fig. 9**   Velocity change in the wake of model at 0 to 20 seconds (X/L=0.5)



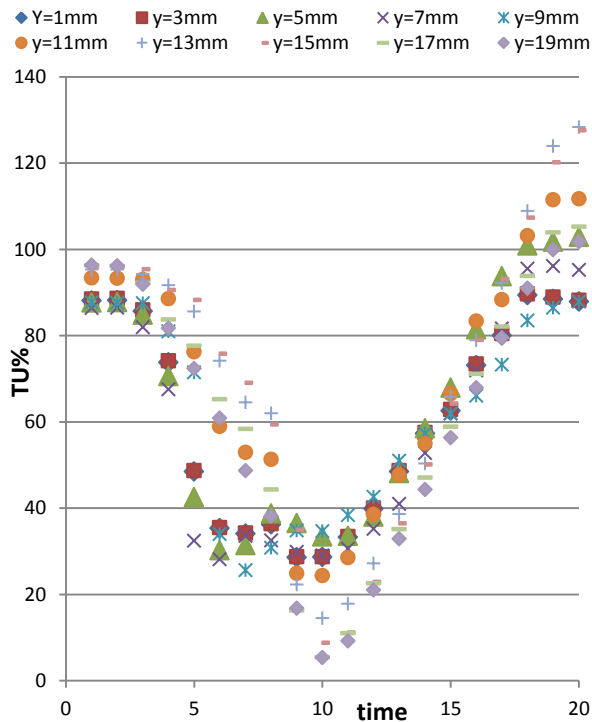**Fig. 10**   Velocity change in the wake of model at 0 to 20 seconds (X/L=1)

**Fig. 11**   Change of turbulence intensity in the wake of
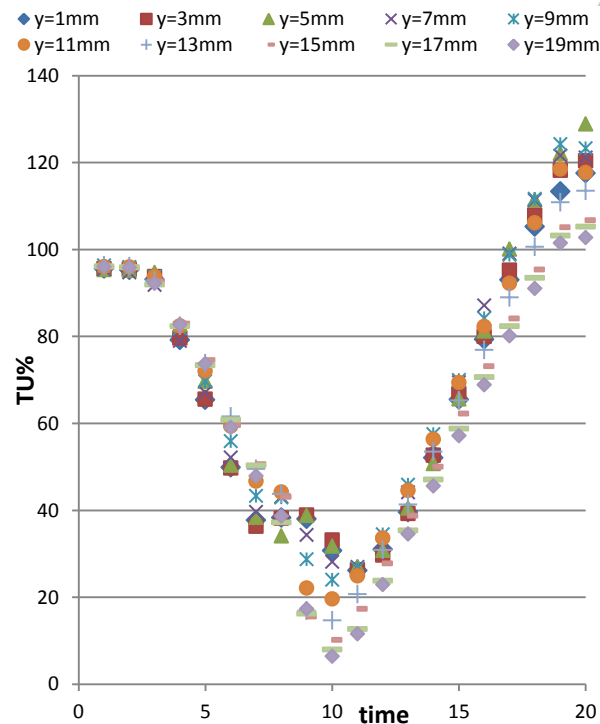model at 0 to 20 seconds (X/L=0.01)



**Fig. 12**   Change of turbulence intensity in the wake of
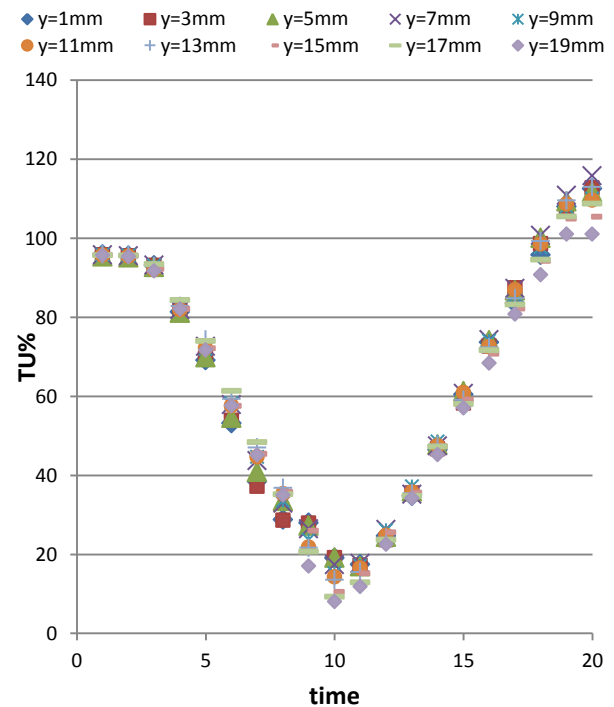model at 0 to 20 seconds (X/L=0.5)



**Fig. 13**   Change of turbulence intensity in the wake of
model at 0 to 20 seconds (X/L=1)

According to the result that is visible, turbulence
intensity level of wake has a downward trend in the
first 10 seconds and this trend is true for different
longitudinal positions. In the 10th second, the
turbulence intensity has an ascending trend. The
velocity changes trend in the wake of car at different
height position and for three length positions is plotted.
With increasing altitude the increasing trend of velocity
is more than farther longitudinal position. In the lower
height the change trend of velocity increased first and
then decreased to reach a value of maxim and again
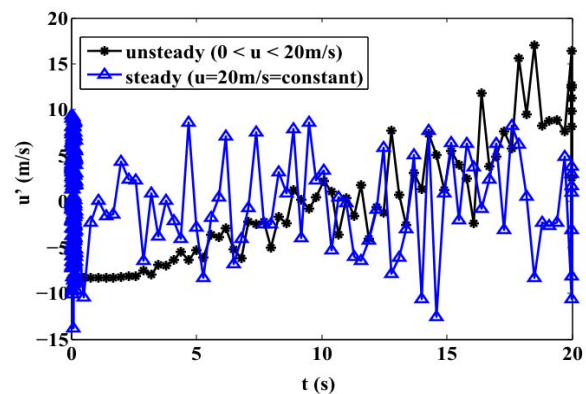increases.



**Fig. 14**   Velocity Fluctuation for steady and unsteady flow
in position (X/L=0.01, y=9mm) at (19.9-20s)

As can be seen from figures 14 to 16, fluctuation velocity for steady and unsteady flow is not equal at the 20th second. Average velocity in the interval (19.9-20s) has been obtained for both flows. The results in Table 1 indicated the amount of unsteady velocity during the periods.
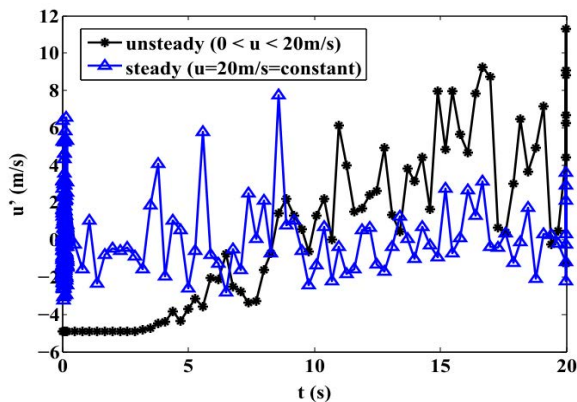


**Fig. 15** Velocity fluctuation for steady and unsteady flow in position (X/L=0.5, y=9mm) at (19.9-20s)
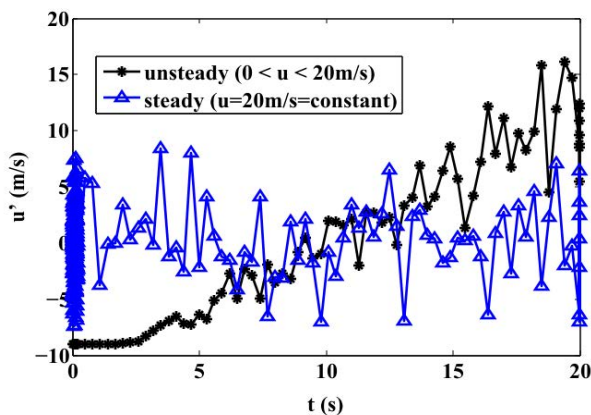


**Fig. 16** Velocity fluctuation for steady and unsteady flow in position (X/L=1, y=9mm) at (19.9-20s)

The instantaneous jumping value can be identified by calculating the value of skewness. In Figures 17-18 it is observed that most of the values of skewness are against zero and have positive and negative values which are indicative of an anisotropic turbulent field in the wake. It is observed in Figure 17 that in the most positions of the wake, in lower height of the wake, the values of skewness are often negative which is indicative of this fact that the instantaneous velocity is lower than average velocity and has maximum jumps. But in the upper heights, the values of skewness are positive and the instantaneous velocity is higher than the average velocity and has fewer minimum jumps compared to it. In the lower and upper heights, the wake peaks of maximum skewness are present and in these parts the extent of mixture is higher and differences in the values of instantaneous velocity with

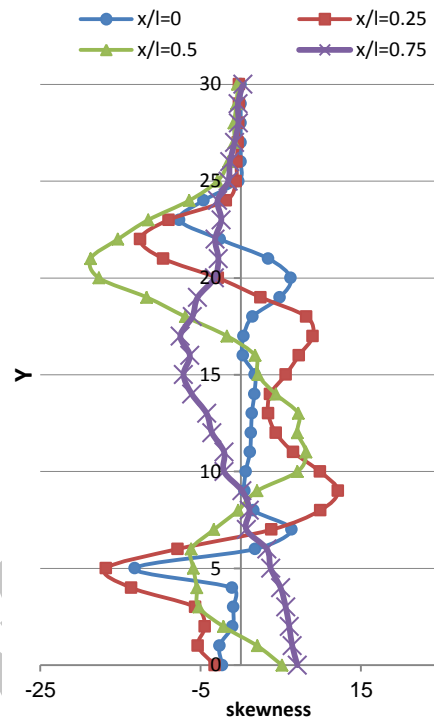the average velocity are more than the other parts in the wake.
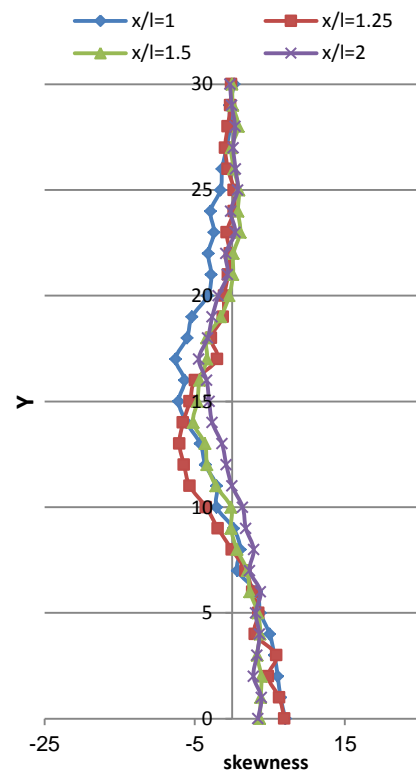


**Fig. 17** Process of change in skewness in the wake of car



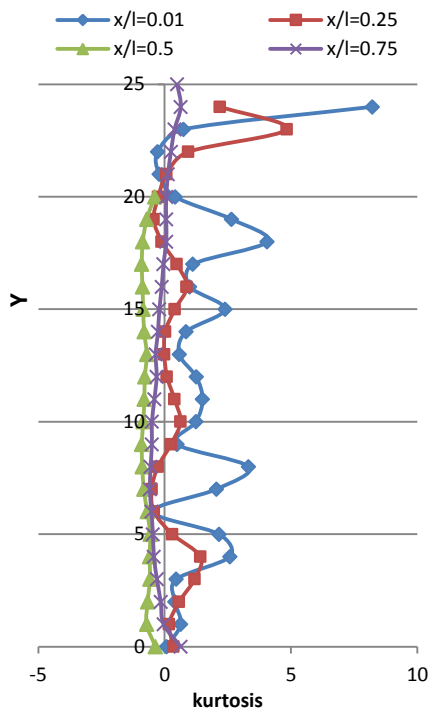**Fig. 18** Process of change in skewness in the wake of car

**Fig. 19**   Process of changes in flatness coefficient in the wake of the car
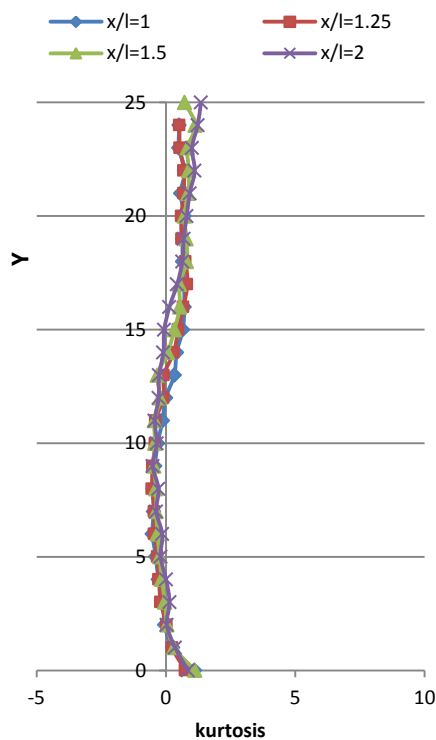


**Fig. 20**   Process of changes in flatness coefficient in the wake of the car

In the middle parts of the wake it is observed that the values of skewness have gradually developed from negative to positive and in the three secondary

positions are rather similar and equal to each other. In Figure 18, we can see that in lower height the values of skewness are positive, but in the middle and upper heights of the behind wake the values of skewness have become negative. In fact, in this range, the values of instantaneous velocity are higher than the average velocity and have fewer minimum peaks than the average velocity. Gradually by distancing from the data gathering position from the car (Figure 6), it is observed that, the values of skewness in the wake are positive. Another worth mentioning point is that with an increase in the wake of the car, the skewness has a downward condition.

Figures 19 to 20 show the process of changes in the kurtosis (flatness coefficient) or the fourth central moment. In Figure 19, for $x/l=0.01$ and $x/l=0.25$ most of the values of kurtosis are positive and the probable density distribution curve is more stretched than the Gaussian density distribution. The instantaneous velocity also in most of the cases distances more from the medium velocity and the jumping and turbulences of the instantaneous velocity of the flow increase. The stretch of the probable distribution density curve for the $x/l=0.01$ states in the lower height of the trail is more tangible where the maximum peaks of kurtosis are observed. The distances of data gathering positions from the car indicates that the values of kurtosis become equal to zero which is indicative of the equality the probable density distribution curve with the normal distribution of Gaussian density. As the distances of most data gathering states from the car increases, it is observed that the probable density distribution curve is still equal to the normal distribution of Gaussian density.
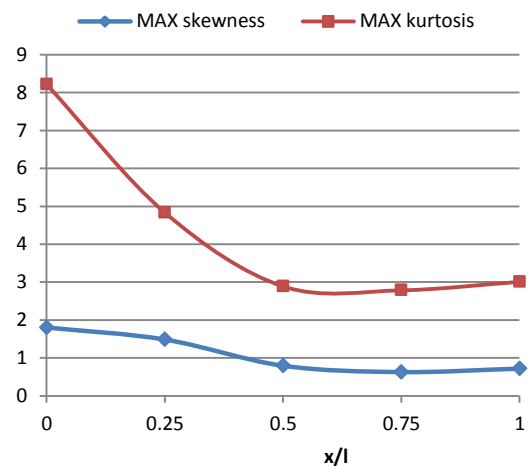


**Fig. 21**   Maximum skewness and kurtosis in the wake of model

Figure 21 shows the maximum skewness and kurtosis for different positions in the back of the car and input velocity of 20m/s. It is clear that with increasing

distance from the model the amount of wake differences reduced and at a far distance the maximum remains constant.
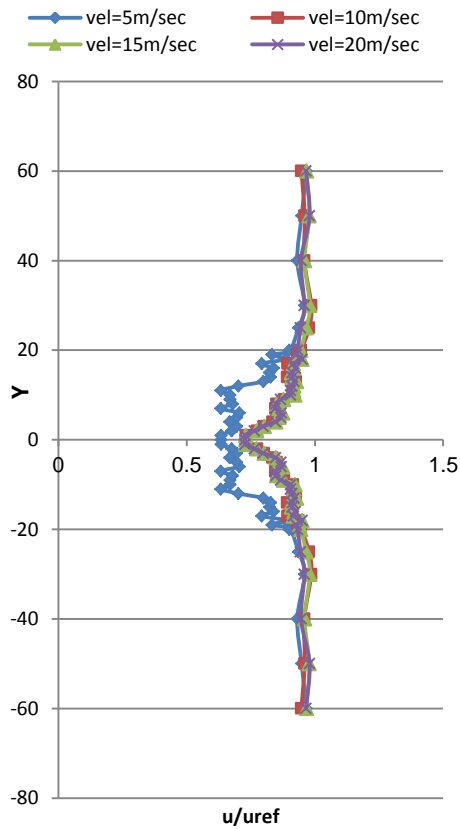


**Fig. 22**  Velocity profile in the wake of car for different inlet velocity
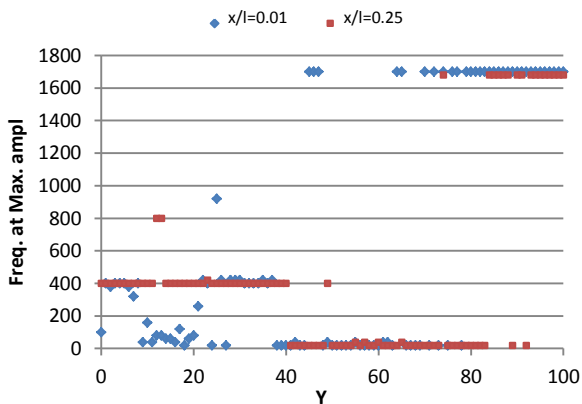


**Fig. 23**  Velocity profile in the wake of car for different inlet velocity

Figure 22 shows the velocity profiles in the wake of the car model at different inlet velocity. It is seen that in the lower speed, velocity in the wake of the car initially is lower and then increased. At the movement initiation due to the low flows peed, Creep-flow occurs and so

the flow in the wake is greater so that with more increasing velocity, the wake of models is forming. With further increasing of vehicle speed, the wake area gradually is reduced and the velocity variations in the sequence are also lessened. Since Karman vortices have highest amplitude, the frequency related to highest amplitude is Karman vortices frequency. Figures 23-26 show the frequency of maximum amplitude at the near model these vortices are formed at lower altitudes and with increasing distance from the model these vortices are formed at higher altitudes.

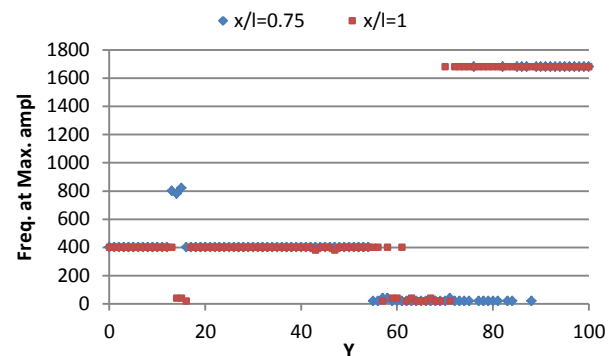

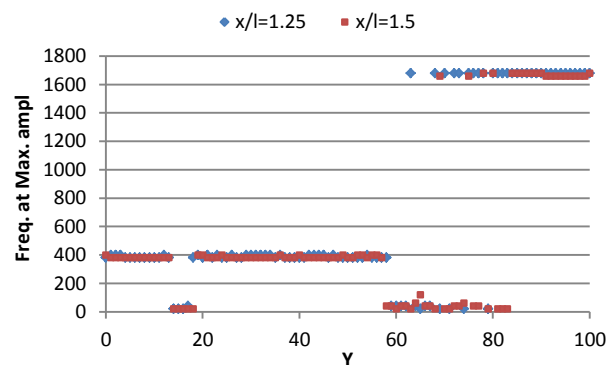**Fig. 24**  Velocity profile in the wake of car for different inlet velocities



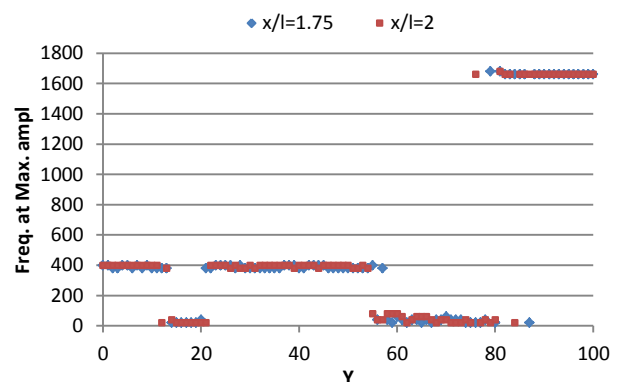**Fig. 25**  Velocity profile in the wake of car for different inlet velocities



**Fig. 26**  Velocity profile in the wake of car for different inlet velocities

Figure 27 shows the change in momentum and Reynolds stress components of drag coefficient and variation of total drag coefficient. For different velocity and with increasing it, the variation trend of momentum term decreased first and then increased. Figure 27 shows that with increasing car speed, velocity in the wake of the car is increasing and this makes that the momentum of control volume (Figure 7) increases and and the momentum term drag coefficient decreases. Gradually, with increasing vehicle speed drag coefficient is fixed.   The maximum value of the momentum term of drag coefficient occurs when the vehicle speed is approximately 5m/sec and then has decreasing trend. At the speed range about 10m/sec to 17.5m/sec the momentum term of drag coefficient is nearly constant. Figure 32 also shows the variation trend of Reynolds stress term of drag coefficient. The Reynolds stress term first decreases and then increases and again decreases.
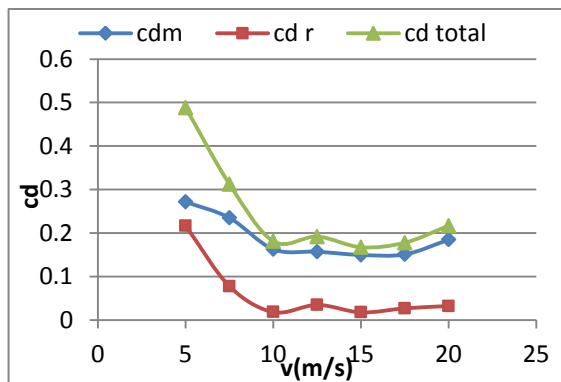


**Fig. 27**   Change trend of drag coefficient and its component with respect to the increasing vehicle speed
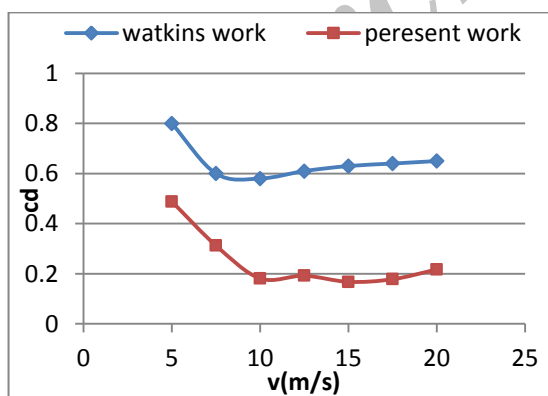


**Fig. 28**   Variation of vehicle drag coefficients trend compared to previous studies

Turbulence is very high at the beginning of motion, and therefore high levels of Reynolds stresses and increasing shear stress caused a sharp increase in the drag coefficient. The Reynolds stress term of drag coefficient at the beginning of motion, is very large and therefore, not to be visible. Therefore, the values of this term are not shown at lower speed. Reynolds stresses in turbulent flow is much larger than laminar flow. Therefore, the values of Reynolds stress term of the drag coefficient are significant in the present work. When the car is moving at a speed of about 10 m/sec the value of this component of the drag coefficient is approximately zero and with further increasing vehicle speed the value of this quantity increases.

Finally, it can be seen that the total drag coefficient at the lower speed is large. It could be due to lack of initial inertia and gradually decreased with increasing vehicle speed. At speed of about 10m/sec the total drag coefficient has its minimum value and with further increasing of vehicle speed at about 20m/sec the drag coefficient reaches at a constant value of about 0.2. It should be noted that the changing trend of drag coefficient in the present work are reasonably consistent with previous work that has been done on a trailer model by ref. [23].

## 6   CONCLUSION

The main results obtained in this study are as follows:

1- Away from the model the velocity and velocity variation are closer to the free flow that may be due to the loss of vortices.
2- At distances close to the model there are three regimes of different flows.
3- At distance near to the model, most of the values of skewness are against zero and have positive and negative values which are indicative of an anisotropic turbulent field in the wake.
4- At low speed of the moving vehicle the velocity in the wake of the model decreases and then increases with the speed rise.
5- The variation trend of momentum term decreased first and then fixed and again increased.
6- the Reynolds stress term first decreases and then increases
7- The total drag coefficient gradually decreased with increasing vehicle speed and at about 10m/sec has its minimum value and with increasing the vehicle speed at about 20m/sec the drag coefficient increased and reached a constant value of about 0.2.

## 8   APPENDIX OR NOMENCLATURE

b:                      Width of model
$C_d$:                      Drag coefficient
h:                      Model height

| | |
|---|---|
| L: | Car length |
| $P_t$: | Total pressure |
| $P_s$: | Static pressure |
| q: | Dynamic pressure |
| $\bar{q}$ : | Mean dynamic pressure |
| Re: | Reynolds number |
| Tu: | Turbulent intensity level |
| U: | Free stream velocity |
| u,v,w: | Velocity component |
| $u', v', w'$ : | Turbulent velocity component |
| x: | Distance from car model |
| ρ: | Density |

## REFERENCES

[1] Barlow, J. B., Rae, W. H., and Pope, A., "Low-Speed Wind Tunnel Testing", John Wiley & Sons, 1999. Kumagai, S., and Isoda, H., Proc. Combust, Inst. 5, 1984, pp. 129-137.

[2] Ahmed, S. R., Ramm, R. and Faltin, G., "Some Salient Features of the Time Averaged Ground Vehicle Wake", SAE Technical Paper Series 840300, Detroit, 1998.

[3] Gilli, P., Chometon, F., "Modelling of Stationary Three-Dimentional Separated Air Flows around an Ahmed Reference Model", Third International Workshop on Vortex, ESAIM Proceedings, Vol. 7, No.10, 1999, pp. 124.

[4] Hanaoka, Y., Kiyohira A., "Vehicle Aerodynamic Development using PAMFLOW", 2003.

[5] Gillieron, P., Spohn, A., "Flow Separations Generated by a Simplified Geometry of an Automotive Vehicle", 2007.

[6] Lienhart, H., Stoocks, C., "Flow and Turbulence Structures in the Wake of a Simplified Car Model (Ahmed Model)", DGLR FachSymp. Der AG STAB, Stuttgart UNIV., 15-17 Nov, 2010.

[7] Khalighi, B., Zang, S., Koromilas, C., Balkanyi, S., Bernal, L. P., Iaccarino, G. and Moin, P., "Experimental and Computational Study of Unsteady Wake Flow behind a Body with a Drag Reduction Device", SAE PPR. 2006-01-1042.

[8] Javareshkiyan, M. H., Shayesteh Sadafiyan, R., and Azarkhish, A., "Numerical and Experimental investigation of Aerodynamics forces on the base model of vehicle", SID, Vol. 18, No. 1, pp. 49-64, (1385 in Persian).

[9] Javareshkiyan, M. H, Zehsaz, M., and Azarkhish, A., "ExprimentalOptimazation of Aerodynamcs forces on the base model of vehicle", 9th Fluid Dynamics Conference, Shiraz University, (Esfand 1383 in Persian).

[10] Watkins, S., Vino, G., "The Effect of Vehicle Spacing on the Aerodynamics of Representative Car Shape", J. of Wind Engineering and Industrial Aerodynamics 96 1232-12393ED., Vol. 96, No. 3, 2011, pp. 1232-1239.

[11] Watkins, S., Vino, G., "The Effect of Vehicle Spacing on the Aerodynamics of Representative Car Shape", J. of Wind Engineering and Industrial Aerodynamics 96 1232-12393ED., Vol. 96, No. 3, 2011, pp. 1232-1239.

[12] Salari. M., Ardakani. M. A., and Taghavi Zonnor. R., "Experimental Study for Effect of Free Flow Temperature Changes and Hot Wire Anemometer on sensors calibration and Velocity measurement", Journal of Mechanics and AeroSpace, Vol. 1, No. 3, 1384, pp. 49-59 (in Persian).

[13] Ardakani, M. A., "Hot Wire Anemometer", Vol. 1, KhajeNasiroddinTosi University, 1385(in Persian).

[14] Morelli, A., "General Layout Characteristic and Performance of a new wind Tunnel for Aerodynamics", SAE Paper No. 710214, Society of Automotive Engineers, Warrendale, Pa., 1971.

[15] Wolf-Heinrich Hucho., "Aerodynamics of Road Vehicles", 4th Edition, SAE, Society of Automotive Engineers Inc Warrendale, Pa, 1998.

[16] Saha, A. K., Muralidhar, K., and Biswas, G. "Experimental Study of Flow Past a Square Cylinder at High Reynolds Numbers", Experiments in Fluids, Vol. 29, No. 4, 2008, pp. 553-563.

[17] Shadaram, A., Azimifrad, M., and Rostami, N., "Study of characteristic flow at the near wake of square cylinder", J. of Mechanical- aerospace Vol. 3, No. 4 1386 in persain.

[18] Goldstein, S., "A Note on the Measurement of Total Head and Static Pressure on a Turbulent Stream", Proceedings of the Royal Society of London, Series A, Vol. 155, No. 32, 1936, pp. 570-575.

[19] LU, B., Bragg, M. B., "Experimental Investigation of the Wake-Survey Method for a Bluff Body with Highly Turbulent Wake", AIAA-3060, 2002.

[20] LU, B., Bragg, M. B., "Experimental Investigation of Airfoil Drag Measurements with Simulated Leading-Edge Ice Using the Wake-Survey Method", AIAA3919, 2000.

[21] LU, B., Bragg, M. B., "Airfoil Drag Measurement with Simulated Leading Edge Ice Using the Wake-Survey Method", AIAA1094, 2003.

[22] Van Dam, C. P., "Recent Experience with Different Methods of Drag Prediction", Progress in aerospace. Science, Vol. 35, No.8, 1999, pp. 751-798.

[23] Chowdhury, H., Moria, H., Iftekhar Khan, A., Alam, F., Watkins, S., "A study on aerodynamic drag of a semi-trailer truck", Procedia Engineering 56, 2013, pp. 201-205.